

Topology optimization for unsteady flows accompanying heat transfers

Suqiong XIE¹⁾, Hiroshi ISAKARI²⁾, Toru TAKAHASHI³⁾, Toshiro MATSUMOTO⁴⁾

- 1) Nagoya University (Furo-cho, Chikusa-ku, Nagoya, Aichi, 464-8601, E-mail: xiesuqiong@nuem.nagoya-u.ac.jp)
 2) Nagoya University (Furo-cho, Chikusa-ku, Nagoya, Aichi, 464-8601, E-mail: isakari@nuem.nagoya-u.ac.jp)
 3) Nagoya University (Furo-cho, Chikusa-ku, Nagoya, Aichi, 464-8601, E-mail: ttaka@nuem.nagoya-u.ac.jp)
 4) Nagoya University (Furo-cho, Chikusa-ku, Nagoya, Aichi, 464-8601, E-mail: t.matsumoto@nuem.nagoya-u.ac.jp)

This paper proposes a topology optimization method for unsteady incompressible viscous fluid flow accompanying heat transfer phenomena, aiming at designing flow channels maximizing the heat transfers. The optimization is performed based on the sensitivities of the objective functional, derived via the adjoint variable method, with respect to design variables (level set function). The lattice kinetic scheme (LKS) is adopted for simulating both the fluid and temperature fields, and the LKS equations for the adjoint functions are derived from the corresponding continuous distribution functions. Numerical examples of channel shape design are presented to demonstrate the validity of the proposed method.

Key Words : Topology optimization, Unsteady flow, Heat transfer, Lattice kinetic scheme, Adjoint method

1. Introduction

Topology optimization is a useful approach to obtain optimum designs using computational techniques in various engineering applications. Since Bendsøe and Kikuchi⁽¹⁾ first proposed the so-called homogenization method for the optimal shape design, lots of methods have been proposed to solve these design problems, such as the solid isotropic material with penalization method⁽²⁾, the level-set method⁽³⁾, etc. The topology optimization problems have also been considered in flow problems, and many methods have also been applied for calculating the optimum fluid fields. The pioneering work for it was done by Borrvall and Petersson⁽⁴⁾ in 2003. Since then, a number of contributions on the topology optimization method for flow field have appeared^(5, 6, 7, 8). Some of them considered the topology optimizations only for steady flows, while a number of publications focused on unsteady flow problems.^(9, 10, 11, 12, 13)

Topology optimization for thermal-fluid coupled problems has attracted much attention in recent years since the thermal-fluid interaction plays an important role in many mechanical systems, such as liquid cooling devices. In 2009, Dede⁽¹⁴⁾ applied the topology optimization method to a fluid-thermal interaction problem, aiming at minimizing the mean temperature, and Yoon et al.⁽¹⁵⁾ proposed a topology optimization method to solve a problem of heat dissipation design. There are many other researches regarding topology optimizations on thermal-fluid coupled problems^(16, 17, 18, 19, 20). These

previous researches have commonly focused on solving thermal fields coupled with steady flows. However, unsteady flow dominates most of the systems in reality. Therefore, this study aims at the development of a topology optimization method considering heat transfer coupled with unsteady incompressible viscous fluid flow.

The finite element method is usually used as the simulation method both for flow and thermal fields in topology optimizations of relevant problems.^(14, 15, 16, 17) In recent years, the lattice Boltzmann method (LBM) has become a popular solver of the Navier-Stokes equation due to its advantages in computational cost and simple algorithm to implement parallel computations. The LBM adopts the discretized time evolution equation of particle velocity distribution functions, which is called the lattice Boltzmann equation (LBE), to compute the probable number of particles at a point of a moment, and the macroscopic variables of fluid, such as density, pressure and velocity, can be obtained from the distribution functions. In 2007, Pinggen et al.⁽²¹⁾ first applied the LBM in topology optimization for fluid flow problems, then the LBM has been applied to different researches of topology optimization methods for fluid flow problems^(22, 23, 24) and fluid-thermal problems^(25, 26).

In 2002, Inamuro proposed the LKS to solve a heat transfer problem by combining the LBM and the kinetic scheme⁽²⁷⁾, and the equilibrium distribution function of the Chapman-Enskog type has been employed in it^(28, 29, 30). The LKS has a simplified LBE, not requiring the computations nor

saving of the distribution functions at every grid in the design domain. Therefore, it can save the computer memory dramatically than the LBM. In addition, the no-slip boundary condition can be directly imposed in the LKS, while the bounce-back condition needs to be considered in the LBM. In this study, we propose the LKS for the simulation of flow field, combining the equilibrium distribution function proposed by He et al.⁽³¹⁾ with that of the LKS. In 2006, a new LKS for heat transfer was derived by Inamuro⁽³²⁾, which is adopted for the modeling of temperature field in this study.

The level-set method is an important approach in topology optimization. The level-set method uses the level set function, a scalar function of point, to express the material distribution in the design domain, and the boundary of the materials can be extracted from the zero-contour of the level set function. The boundary shape of the fluid domain is changed in accordance with the updating of the distribution of the level set function during the optimization. Following the method proposed by Yamada et al.⁽³³⁾ and Yaji et al.,⁽²⁵⁾ we employ the level-set method to distinguish the fluid and solid domains, and use the reaction-diffusion equation to update the level set function. The reaction-diffusion equation has the design sensitivity term, which is calculated by introducing the adjoint functions of the LKS for fluid field and temperature field. In this study, the adjoint functions are derived following the method proposed by Yaji et al.^(34, 25)

In the following sections of this article, Section 2.1 introduces the forward modeling of fluid field and temperature field using the LKS, Section 2.2 describes the optimization problem, Section 2.3 illustrates level-set method, and Section 2.4 shows the derivation of the adjoint functions as well as the design sensitivity. Section 3 introduces the computation algorithm of the proposed topology optimization method. Numerical examples are presented in Section 4 to demonstrate the effectiveness of this method.

2. Problem formulation

2.1. Forward modeling

In this study, we use dimensionless variables defined by a reference temperature \hat{T} , a reference density $\hat{\rho}_0$, a characteristic length \hat{L} , a characteristic particle speed \hat{c} , and a characteristic time scale $\hat{t}_0 = \hat{L}/\hat{U}$, where \hat{U} is a characteristic flow speed.

2.1.1. Fluid field modeling

In the LKS proposed by Inamuro⁽²⁷⁾, the velocity \mathbf{u} and the pressure p of the fluid at the point \mathbf{x} and time t are calculated as follows:

$$p(\mathbf{x}, t) = \frac{1}{3} \sum_{i=1}^N f_i^{\text{eq}}(\mathbf{x} - \mathbf{c}_i \Delta x, t - \Delta t), \quad (1)$$

$$\mathbf{u}(\mathbf{x}, t) = \frac{1}{\rho_0} \sum_{i=1}^N \mathbf{c}_i f_i^{\text{eq}}(\mathbf{x} - \mathbf{c}_i \Delta x, t - \Delta t), \quad (2)$$

where f_i^{eq} is the equilibrium distribution function defined below, N is the number of discretized directions, Δx is a lattice spacing, and Δt is the time step during which the fictive particles travel one lattice spacing.

We adopt the D2V9 lattice model shown in Fig. 1 in this study. This model restricts the particles' velocity in 9 directions in the plane space, i.e., $N = 9$. In the D2V9 lattice model, the velocity vectors $\mathbf{c}_{i=1,\dots,9}$ of the particles are defined as

$$[\mathbf{c}_1, \mathbf{c}_2, \mathbf{c}_3, \mathbf{c}_4, \mathbf{c}_5, \mathbf{c}_6, \mathbf{c}_7, \mathbf{c}_8, \mathbf{c}_9] = \begin{bmatrix} 0 & 1 & 0 & -1 & 0 & 1 & -1 & -1 & 1 \\ 0 & 0 & 1 & 0 & -1 & 1 & 1 & -1 & -1 \end{bmatrix}. \quad (3)$$

In 1997, a new LBM model was proposed by He et al.⁽³¹⁾ treating the fluid density ρ_0 as a constant to reduce the compressible influence of the LBM. Following He et al.,⁽³¹⁾ we use the equilibrium distribution function f_i^{eq} expressed as

$$f_i^{\text{eq}} = w_i \left\{ 3p + \rho_0 \left[3c_{i\gamma} u_\gamma + \frac{9}{2} c_{i\gamma} c_{i\beta} u_\gamma u_\beta - \frac{3}{2} u_\gamma u_\gamma + A \Delta x \left(\frac{\partial u_\beta}{\partial x_\gamma} + \frac{\partial u_\gamma}{\partial x_\beta} \right) c_{i\gamma} c_{i\beta} \right] \right\}, \quad (4)$$

with $\rho_0 = 1.0$. In Eq.(4), β and γ , ($= x$ or y), represent components of Cartesian coordinates, where the summation convention is applied for repeated indices of Greek letters. w_i is the weight coefficient given by

$$w_i = \begin{cases} \frac{4}{9} & i = 1 \\ \frac{1}{9} & i = 2, 3, 4, 5 \\ \frac{1}{36} & i = 6, 7, 8, 9. \end{cases}, \quad (5)$$

and A is a constant parameter of $O(1)$ determining the kinematic viscosity coefficient ν of the fluid by

$$\nu = \left(\frac{1}{6} - \frac{2}{9} A \right) \Delta x. \quad (6)$$

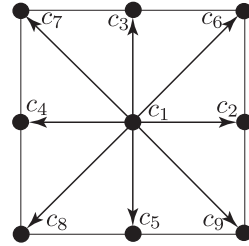


Fig. 1 D2V9 model.

In the LBM, we usually apply the bounce-back boundary condition in terms of the velocity distribution function. However in the LKS, the macroscopic variables can be directly specified on the boundaries. Therefore, the LKS has an additional advantage that we can use the same boundary conditions as those in the usual CFD simulations.

2.1.2. Temperature field modeling

In 2006, Inamuro⁽³²⁾ developed an LKS for the modeling of temperature field, in which the equilibrium distribution function h_i^{eq} with respect to the temperature field reads

$$h_i^{\text{eq}} = w_i T (1 + 3c_{i\gamma} u_\gamma) + w_i B \Delta x c_{i\gamma} \frac{\partial T}{\partial x_\gamma}, \quad (7)$$

with a constant parameter B determining the thermal diffusivity α by

$$\alpha = \left(\frac{1}{6} - \frac{1}{3}B \right) \Delta x. \quad (8)$$

The temperature T and the heat flux \mathbf{q} are computed by

$$T(\mathbf{x}, t) = \sum_{i=1}^9 h_i^{\text{eq}}(\mathbf{x} - \mathbf{c}_i \Delta x, t - \Delta t), \quad (9)$$

$$\mathbf{q}(\mathbf{x}, t) = \sum_{i=1}^N \mathbf{c}_i h_i^{\text{eq}}(\mathbf{x} - \mathbf{c}_i \Delta x, t - \Delta t) - T \mathbf{u}(\mathbf{x}, t). \quad (10)$$

The first derivatives $\frac{\partial u_\beta}{\partial x_\gamma}$ and $\frac{\partial T}{\partial x_\gamma}$ in Eq. (4) and Eq. (7) are calculated through the finite-difference approximations⁽²⁷⁾, as follows:

$$\frac{\partial u_\beta}{\partial x_\gamma} \approx \frac{1}{6\Delta x} \sum_{i=1}^9 c_{i\gamma} u_\beta(\mathbf{x} + \mathbf{c}_i \Delta x), \quad (11)$$

$$\frac{\partial T}{\partial x_\gamma} \approx \frac{1}{6\Delta x} \sum_{i=1}^9 c_{i\gamma} T(\mathbf{x} + \mathbf{c}_i \Delta x). \quad (12)$$

2.1.3. Initial and boundary conditions

As shown in Fig. 2, Ω , $\partial\Omega$, and $\bar{\Omega}$ denote the fluid domain, its boundary, and the solid domain, respectively. On the boundary Γ_v , the fluid velocity is prescribed as $\mathbf{u} = \mathbf{u}_{\text{in}}$ and the temperature is given as T_{in} . On the boundary Γ_p , the prescribed pressure is given as $p = p_{\text{out}}$ and the adiabatic boundary condition is applied. \mathbf{n}_p represents the unit outward normal vector of the design domain and Γ_A represent adiabatic boundary excluding Γ_p . The boundary conditions are summarized as follows:

$$\left. \begin{array}{ll} \mathbf{u} = \mathbf{u}_{\text{in}} & \text{on } \Gamma_v \\ p = p_{\text{out}} & \text{on } \Gamma_p \\ \mathbf{u} = \mathbf{0} & \text{on } \Gamma_w \cup \partial\Omega \\ T = T_{\text{in}} & \text{on } \Gamma_v \\ \mathbf{n}_p \cdot \nabla T = 0 & \text{on } \Gamma_p \cup \Gamma_A \end{array} \right\}. \quad (13)$$

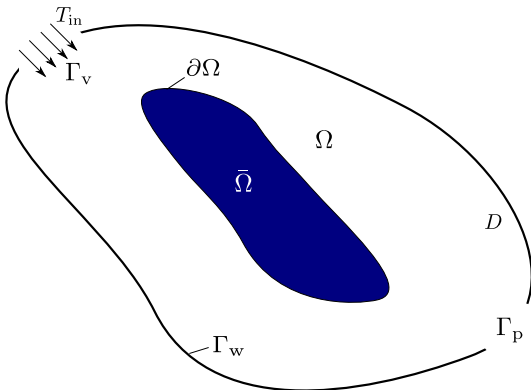


Fig. 2 Problem setting.

At the initial time of optimization, the velocity \mathbf{u} and the temperature T in the design domain D are given as

$$\mathbf{u} = \mathbf{u}(\mathbf{x}, 0) = (u_0, 0), \quad (14)$$

$$T = T(\mathbf{x}, 0) = T_0. \quad (15)$$

2.2. Optimization problem

The topology optimization problems for unsteady flows can be written as

$$\inf_{\phi} J = \int_I \int_D Z(\mathbf{u}, p, T) dD dt, \quad (16)$$

$$\text{s.t. } V = V_\Omega - V_{\text{max}} \leq 0, \quad (17)$$

where J is the objective functional computed by integrating a certain functional $Z(\mathbf{u}, p, T)$ over the design domain D and a time space I , $t \in I$; V is the volume constraint restricting the volume of the fluid field V_Ω of the optimized shape with the volume constraint V_{max} .

2.3. Level-set based optimization

In level-set method, the level set function ϕ , a scalar function of point, is employed to express the material distribution. ϕ is defined as

$$\begin{cases} 0 < \phi(\mathbf{x}) \leq 1 & \text{if } \mathbf{x} \in \Omega, \\ \phi(\mathbf{x}) = 0 & \text{if } \mathbf{x} \in \partial\Omega, \\ -1 \leq \phi(\mathbf{x}) < 0 & \text{if } \mathbf{x} \in \bar{\Omega}. \end{cases} \quad (18)$$

The boundary of the fluid domain can be extracted from the iso-surface of $\phi(\mathbf{x})$ corresponding to $\phi(\mathbf{x}) = 0$.

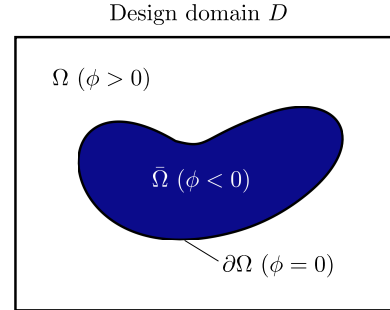


Fig. 3 Level set method.

Thus, we define the characteristic function⁽³³⁾ χ_ϕ as

$$\chi_\phi(\mathbf{x}) = \begin{cases} 1 & \text{if } \phi(\mathbf{x}) \geq 0 \Leftrightarrow \mathbf{x} \in (\Omega \cup \partial\Omega), \\ 0 & \text{if } \phi(\mathbf{x}) < 0 \Leftrightarrow \mathbf{x} \in \bar{\Omega}. \end{cases} \quad (19)$$

The volume of the fluid field is then calculated by

$$V_\Omega = \int_D \chi_\phi d\Omega. \quad (20)$$

Following Yamada et al.⁽³³⁾, we employ the following reaction-diffusion equation to update $\phi(\mathbf{x})$ during the optimization

$$\frac{\partial \phi}{\partial \zeta} = -K(J' - \tau_R \nabla^2 \phi), \quad (21)$$

where ζ is fictitious time, $K > 0$ is a constant, and J' denotes the design sensitivity. Also, $\tau_R \nabla^2 \phi$ is the regularization term controlling the complexity of the shape of the fluid domain.

The boundary of the fluid domain is changed in accordance with the updating of the distribution of the value of ϕ during the optimization.

2.4. Variations of the objective functional

In the research by Yaji et al.⁽³⁴⁾, the level set function ϕ is introduced to the equilibrium distribution function by replacing \mathbf{u} with $\phi\mathbf{u}$ as below:

$$\mathbf{u} := \phi\mathbf{u}. \quad (22)$$

Similarly, we introduce ϕ to the equilibrium distribution functions in the LKS, and derive the design sensitivity by the adjoint method. First, we define the augmented objective functional \bar{J} as follows:

$$\bar{J} = J + G + \lambda V, \quad (23)$$

$$G = G_1 + G_2, \quad (24)$$

$$G_1 = \int_D \int_I \int_{\mathbb{R}^2} \tilde{f} \left\{ \frac{\partial f}{\partial t} + \mathbf{c} \cdot \nabla f + \frac{1}{\tau_f} (f - f^{\text{eq}}) \right\} d\mathbf{c} dt dD = 0, \quad (25)$$

$$G_2 = \int_D \int_I \sum_{i=1}^9 \tilde{h}_i \left\{ \frac{\partial h_i}{\partial t} + \mathbf{c}_i \cdot \nabla h_i + \frac{1}{\tau_h} (h_i - h_i^{\text{eq}}) \right\} dt dD = 0, \quad (26)$$

where τ_f and τ_h are the relaxation times, \mathbb{R}^2 is the velocity space and $\mathbf{c} \in \mathbb{R}^2$. $\tilde{f}(\mathbf{x}, \mathbf{t}, t)$, $\tilde{h}_i(\mathbf{x}, t)$ and λ are the Lagrange multipliers, where $\lambda \geq 0$.

In G_1 the continuous Boltzmann equation with Bhatnagar-Gross-Krook collision operator is employed, from which \tilde{f} is derived and then discretized using the LKS. In G_2 the lattice Boltzmann equation for temperature field is employed, from which \tilde{h} is derived and then extended to the LKS.

Following Yaji et al.^(25, 34), \tilde{f} is derived and discretized as follows:

$$\begin{aligned} & \tilde{f}_i(\mathbf{x} - \mathbf{c}_i \Delta \mathbf{x}, t - \Delta t) - \tilde{f}_i^{\text{eq}}(\mathbf{x}, t) \\ & - 3T \sum_{j=1}^9 w_j \tilde{h}_j \mathbf{c}_j \cdot (\mathbf{c}_i - \mathbf{u}) - \delta_{f_i} Z = 0, \end{aligned} \quad (27)$$

where $\delta_{f_i} Z$ is the variation of Z with respect to f_i , and \tilde{f}_i^{eq} is defined as

$$\tilde{f}_i^{\text{eq}} = \sum_{j=1}^9 \tilde{f}_j f_j^a \{1 + 3(\mathbf{c}_i - \mathbf{u}) \cdot (\mathbf{c}_j - \mathbf{u})\}, \quad (28)$$

with f_j^a , ($j = 1, \dots, 9$) defined as

$$f_j^a = w_j \left(1 + 3c_{j\gamma} u_\gamma + \frac{9}{2} c_{j\gamma} c_{j\beta} u_\gamma u_\beta - \frac{3}{2} u_\gamma u_\gamma \right), \quad (29)$$

and \tilde{h} is derived as follows

$$\tilde{h}_i(\mathbf{x} - \mathbf{c}_i \Delta \mathbf{x}, t - \Delta t) - \tilde{h}_i^{\text{eq}}(\mathbf{x}, t) - \delta_{h_i} Z = 0, \quad (30)$$

where $\delta_{h_i} Z$ is the variation of Z with respect to h_i , and \tilde{h}_i^{eq} is defined as

$$\tilde{h}_i^{\text{eq}} = \sum_{j=1}^9 w_j \tilde{h}_j (1 + 3\mathbf{c}_i \cdot \mathbf{u}). \quad (31)$$

We find that the time progress in the adjoint functions Eq. (27) and Eq. (30) are reversed. Therefore, in order to solve them, they have to be calculated from the final time to the initial time. For the value of the adjoint functions at initial time step, i.e., the final time step of the forward modeling, we can assume

$$\tilde{h}_i = 0, \quad (32)$$

$$\tilde{f}_i = 0. \quad (33)$$

Consequently, the design sensitivity $\delta_\phi \bar{J}$ is derived as

$$\begin{aligned} \delta_\phi \bar{J} = & \int_D \left\{ \int_I \left\{ \sum_{i=1}^9 3\tilde{f}_i w_i \right. \right. \\ & \times \left[3p + \rho_0 \left(3c_{i\gamma} u_\gamma + \frac{9}{2} c_{i\gamma} c_{i\beta} u_\gamma u_\beta - \frac{3}{2} u_\gamma u_\gamma \right) \right] \\ & \left. \left. \times (u_\gamma u_\gamma - c_{i\gamma} u_\gamma) + 3T \sum_{i=1}^9 \tilde{h}_i w_i c_{i\gamma} u_\gamma \right\} dt + \lambda \right\} \delta\phi d\Omega. \end{aligned} \quad (34)$$

The $\delta_\phi \bar{J}$ is used as J' in Eq. (21) when the design domain is discretized with unit squares, and based on Eq. (21) the optimization is performed.

3. Computation algorithm

During the optimization, the objective functional is considered to be converged when it satisfies the following criterion:

$$\frac{|J_m - J_{m-1}|}{J_{m-1}} \leq \epsilon, \quad (35)$$

where m denotes the step number of the optimization process.

The computation algorithm of the present optimization procedure is shown as follows:

- (i) Initialize the values of ϕ , \mathbf{u} , p , and T in the design domain D .
- (ii) Compute the fluid field and temperature field using the LKS, and store the macroscopic variables \mathbf{u} , p , and T at all time steps.
- (iii) Calculate the objective functional. If both Eq. (35) and Eq. (17) are satisfied, terminate the computation. Otherwise go to (iv).
- (iv) Calculate the adjoint functions and the design sensitivity J' .
- (v) Update ϕ using Eq. (21), and go back to (ii).

4. Numerical examples

In this study, the value of ϕ at initial time is given as $\phi_{t=0} = 1.0$ in the fluid domain and $\phi_{t=0} = -1.0$ on the wall of the design domain, i.e., the design domain is fully filled with fluid at the initial time. The Reynolds number Re and Prandtl number Pr are defined as

$$Re = \frac{U_m L}{\nu}, \quad (36)$$

$$Pr = \frac{\nu}{\alpha}, \quad (37)$$

where U_m is the mean velocity on Γ_v , L is the representative length of Γ_v . For the unsteady flow optimization, the prescribed velocity on Γ_v is given as $\mathbf{u}_{in} = (U, 0)$, where

$$U = \frac{4u_{\max}(y_1 - y)(y - y_2)}{(y_1 - y_2)^2}(\sin(\omega t) + 1.0), \quad (38)$$

and y_1 and y_2 are the coordinates of y -axis of the upper and bottom ends of Γ_v , ω is the angular frequency of the inflow velocity. In the maximization problems, a minus sign is added to the objective functional so that it can be treated as a minimization problem. In the figures showing the flow field configurations during the optimization process, the blue regions represent the solid ones and the white regions represent the fluid areas.

4.1. Maximization of the temperature of the fluid domain

In this section, we attempt to maximize the average temperature of the fluid domain, in which two heating boundaries are symmetrically located at the center of the upper and bottom walls of the design domain. The objective functional is defined as

$$\inf_{\phi} J = -\frac{1}{N_t V_D} \int_{\Omega} \sum_{n=0}^{N_t} T^2 d\Omega, \quad (39)$$

where n is time step in the forward modeling, $n \in \{0, \dots, N_t\}$, and V_D is the volume of the design domain.

The design domain is shown in Fig. 4 and is discretized into $90\Delta x \times 90\Delta x$. The inlet boundary Γ_v is on the left side of the design domain, where the prescribed velocity is given as $U_m = 0.012$. The pressure on Γ_p is given as $p_{out} = \frac{1}{3}$. The walls of the design domain are adiabatic except the heating areas where their temperatures are kept constant as $T_s = 5.0$. The solid materials introduced to the design domain during the optimization are adiabatic, and on the boundary Γ_A of these solid materials the adiabatic boundary condition is applied. The temperature on Γ_v is given as $T_{in} = 1.0$, and we set the temperature of the initial design domain as $T_0 = 1.0$ and $N_t = 6000$. The volume constraint is $V_{\max} = 0.80V_0$, and we assume as $Re = 10$ and $Pr = \frac{1}{3}$.

Firstly, we set the inflow frequency as $\omega = \frac{\pi}{1500}$. The initial configuration of the design domain before optimization is shown in Fig. 5(a) and the obtained optimized configuration is shown in Fig. 5(b).

The average temperature distributions are shown in Fig. 6, from which we find, in the optimized configuration, the solid materials lead the fluid to the heat sources so that the fluid can be heated efficiently. Also, the velocity vectors at different time in the optimized channel are shown in Fig. 7.

The histories of the objective functional values and the volumes of the fluid area are shown in Fig. 8, in which the values of the volumes are normalized as V_{Ω}/V_0 , where V_{Ω} and V_0 are the volumes of the optimized and initial fluid regions, respectively. The objective and volume values converged after 160th iteration step of the optimization. Fig. 9 shows the configurations at different iteration steps. The solid material appears near the inlet first to guide the flow

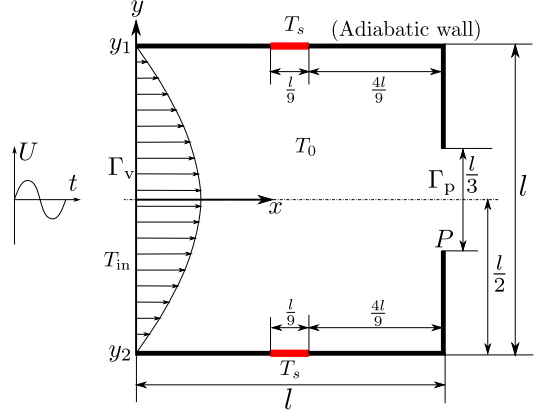


Fig. 4 Design domain for the maximization of temperature in the fluid domain.

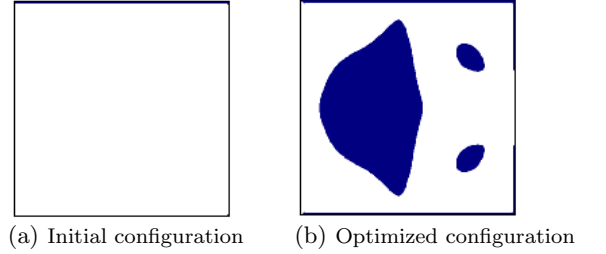


Fig. 5 The optimized configuration in maximizing the temperature of the fluid domain in the case of $\omega = \frac{\pi}{1500}$.

to the heating boundaries. After it grows, solid materials are generated near the outlet, spreading the heat transfer in the fluid domain.

4.1.1. Dependence of the optimization results on the inflow frequencies

Now we demonstrate the influence of the inflow frequencies by testing for $\omega = \frac{\pi}{3000}$, $\frac{\pi}{1500}$, $\frac{\pi}{750}$, and $\frac{\pi}{375}$. The optimized configurations for different values of ω are shown in Fig. 10, from which we find that the optimized configurations slightly depend on the choice of ω . The objective functional and the volume values are compared in Table 1, where J and J_0 are the objective functional values for the optimized and initial configurations, while V_{Ω} and V_0 are the fluid volumes of the optimized and initial configurations, respectively.

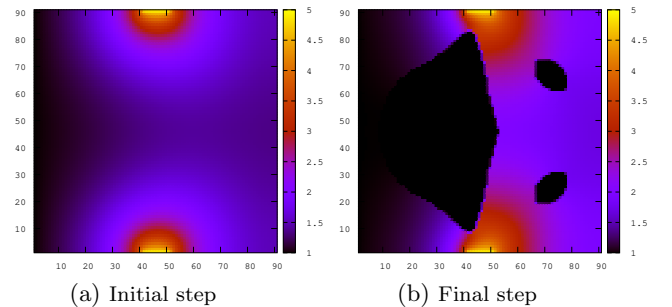


Fig. 6 The average temperature distribution obtained in the example of maximizing the temperature.

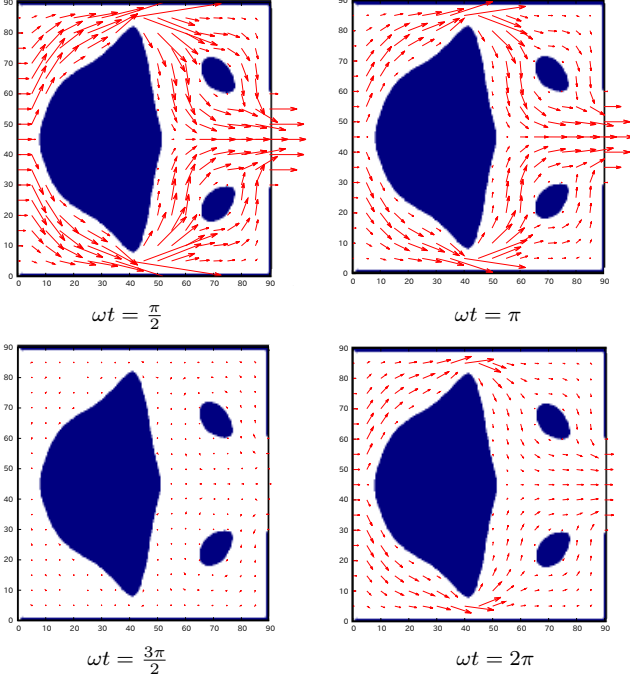


Fig. 7 The velocity vector fields at different time of the optimized configurations for maximizing the temperature of the fluid domain ($\omega = \frac{\pi}{1500}$).

4.2. Maximization of the heat transfer between solid and fluid domains

In this section, we consider a problem of maximizing the heat transfer between the solid and fluid domains. Following Dugast et al. (26), we use the objective functional for aiming at maximizing the heat evacuated by the fluid flow, given as follows:

$$\inf_{\phi} J = -\frac{1}{N_t l_{\Gamma_p}^2} \int_{\Gamma_p} \sum_{n=0}^{N_t} [(\mathbf{n}_p \cdot \mathbf{u})T]^2 d\Gamma_p,$$

where l_{Γ_p} represents the width of Γ_p .

The design domain is depicted in Fig. 11. The velocity-prescribed boundary Γ_v is set on the left-side of the design domain and we assume the inflow frequency $\omega = \frac{\pi}{1500}$. The

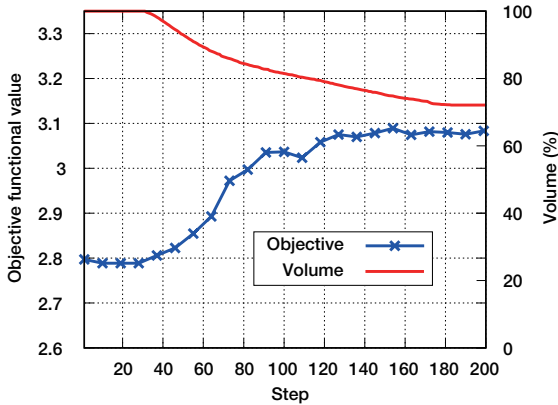


Fig. 8 The histories of the objective functional and volume values in maximizing the temperature for the case of $\omega = \frac{\pi}{1500}$.

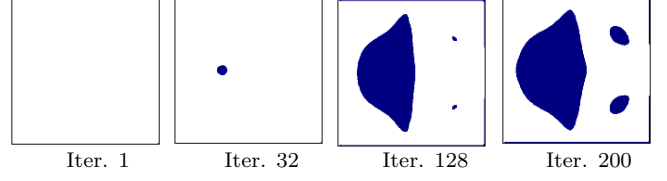


Fig. 9 The configurations of the materials generated at different iteration steps of optimization.

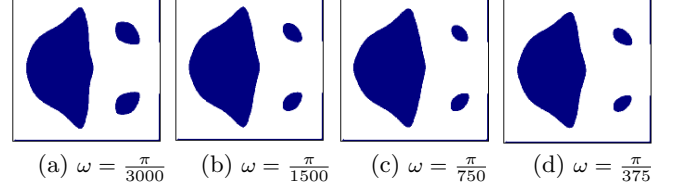


Fig. 10 Optimized configurations of the generated materials in maximizing the average temperature for different ω .

pressure-prescribed boundary Γ_p is on the right-side of the design domain, and we assume $p_{out} = \frac{1}{3}$, $T_{in} = 1.0$, $T_0 = 1.0$, and $N_t = 6000$. In this example, the temperatures of the walls of the design domain and the generated solid material are given as $T_s = 5.0$ and kept unchanged during the optimization. Therefore, the heat energy is supplied from the design domain walls and the solid materials. Also, the Reynolds number and the Prandtl number are assumed as $Re = 20.0$ and $Pr = \frac{5}{9}$, respectively, while the volume constraint is given as $V_{max} = 0.70V_0$. Moreover, the solid material is assumed to have the same thermal properties as that of the fluid.

The design domain is discretized into $120\Delta x \times 120\Delta x$. The initial and optimized configurations are shown in Fig. 12(a) and Fig. 12(b), respectively, and the distribution of the velocity vectors calculated at $\omega t = 2\pi$ are shown in Fig. 13. We find that the flow is divided into two streams so that the fluid can be heated by the solid part efficiently. This can also be understood from the distribution of the average temperature $\sum_{n=0}^{N_t} T/N_t$ in the design domain, as shown in Fig. 14. The histories of the values of the objective functional and solid volumes are shown in Fig. 15, where the objective functional value is normalized as J/J_0 .

We find that the objective functional value increases in accordance with the generation of the solid materials in the design domain. Then, we observe its up-and-down changed caused by sudden changes in topology and shape of the solid material distribution, and it converges after 500 iteration steps of the optimization. The value of the objective function becomes 4.64 times greater than that of the initial step, and the volume of the fluid area is reduced to 50.62% of that of the initial step.

5. Conclusions

This paper has presented a topology optimization method for unsteady incompressible viscous fluid flows accompany-

Table 1: Comparison between the objective functional and solid volume values obtained for different ω .

ω	J	J_0	V_{Ω}/V_0
$\pi/3000$	3.34	2.81	71.40
$\pi/1500$	3.08	2.79	72.12
$\pi/750$	3.03	2.77	72.21
$\pi/375$	2.98	2.77	72.31

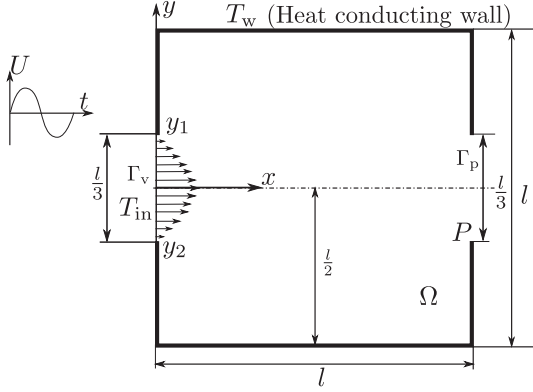


Fig. 11 Design domain for maximizing heat transfer.

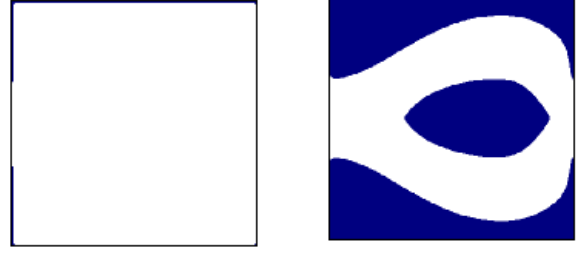
ing with heat transfers, based on level-set method for material distribution modeling and the LKS for flow field computation. The adjoint equations for the distribution functions of the LKS have been derived. Also, the variations of the objective functional in terms of adjoint distribution functions for the flow velocity and the temperature have been derived. The numerical examples have demonstrated the proposed method can solve topology optimization problems for unsteady flows accompanying heat transfers effectively. The proposed approach can be one of the effective tools of shape designs of flow channels considering heat transfer problems for unsteady flows.

Acknowledement

The authors are grateful to the reviewers' valuable comments that improved significantly the manuscript.

References

- (1) M.P. Bendsøe and N. Kikuchi, Generating optimal topologies in structural design using a homogenization method, *Computer methods in applied mechanics and engineering*, Vol. 71, No. 2, (1988), pp. 197–224.
- (2) M.P. Bendsøe, Optimal shape design as a material distribution problem, *Structural Optimization*, Vol. 1, (1989), pp. 193–202.
- (3) M. Wang, X. Wang, and D. Guo, A level set method for structural topology optimization, *Computer Methods in Applied Mechanics and Engineering*, Vol. 192, (2003), pp. 227–246.



(a) Initial configuration

(b) Optimized configuration

Fig. 12 The optimized configurations of solid materials for maximizing heat transfer.

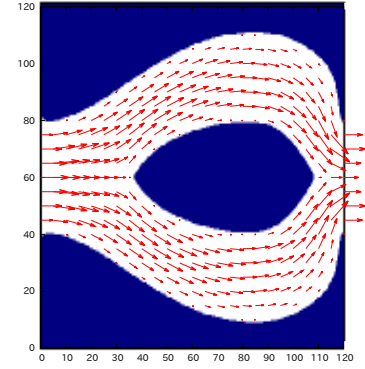


Fig. 13 The velocity vector distribution for the optimized configurations of solid materials for maximizing heat transfer calculated at $\omega t = 2\pi$.

- (4) M. Borrvall and J. Petersson, Topology optimization of fluids in Stokes flow, *International journal for numerical methods in fluids*, Vol. 41, No. 1, (2003), pp. 77–107.
- (5) A. Gersborg-Hansen, O. Sigmund, and R. Habor, Topology optimization of channel flow problems, *Structural and Multidisciplinary Optimization*, Vol. 30, (2004), pp. 181–192.
- (6) S. Kreissl, G. Pingen, A. Evgrafov, and K. Maute, Topology optimization of flexible micro-fluidic devices, *Structural and Multidisciplinary Optimization*, Vol. 42, (2010), pp. 495–516.
- (7) N. Aage, Poulsen, H. Thomas, A. Gersborg-Hansen, and O.A. Sigmund, Topology optimization of large scale Stokes flow problems, *Structural and Multidisciplinary Optimization*, Vol. 35, (2008), pp. 175–180.
- (8) S. Zhou and Q. Li, A variational level set method for the optimization of steady-state Navier-Stokes flow, *Journal of Computational Physics*, Vol. 227, (2008), pp. 10178–10195.
- (9) S. Kreissl, G. Pingen, and K. Maute, Topology optimization for unsteady flow, *International Journal of Numerical Methods in Engineering*, Vol. 87, (2011), pp. 1229–1253.
- (10) Y. Deng, Z. Liu, P. Zhang, Y. Liu, and Y. Wu, Topology optimization of unsteady incompressible

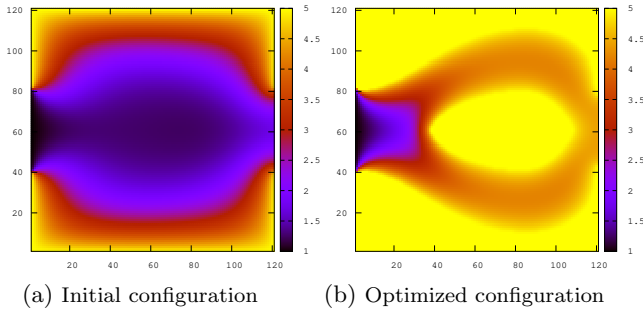


Fig. 14 The distribution of average temperature obtained for maximizing the heat transfer.

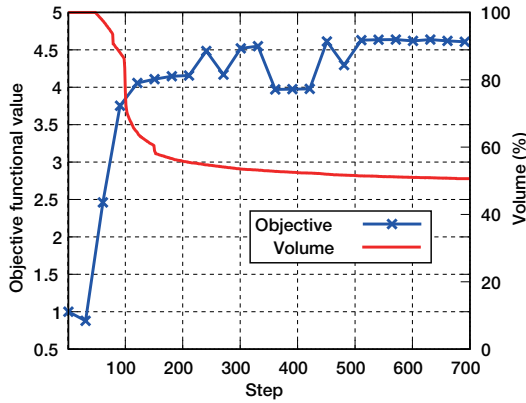


Fig. 15 The history of the values of the objective functional and the volume of the solid materials in maximizing heat transfer.

Navier-Stokes flows, *Journal of Computational Physics*, Vol. 230, No. 17, (2011), pp. 6688–6708.

- (11) S. Nørgaard, O. Sigmund, and B. Lazarov, Topology optimization of unsteady flow problems using the lattice Boltzmann method, *Journal of Computational Physics*, Vol. 307, (2016), pp. 291–307.
- (12) C. Chen, K. Yaji, T. Yamada, K. Izui, and S. Nishiwaki, Local-in-time adjoint-based topology optimization of unsteady fluid flows using the lattice Boltzmann method, *Mechanical Engineering Journal*, Vol. 4, No. 3, (2017), pp. 17-00120.
- (13) T. Nguyen, H. Isakari, T. Takahashi, K. Yaji, M. Yoshino, and T. Matsumoto, Level-set based topology optimization of transient flow using lattice Boltzmann method considering an oscillating flow condition, *Computers and Mathematics with Applications*, Vol. 80, (2020), pp. 82–108.
- (14) E. Dede, Multiphysics topology optimization of heat transfer and fluid flow systems, *Proceedings of the COMSOL Conference 2009 Boston*, (2009).
- (15) G.H. Yoon, Topological design of heat dissipating structure with forced convective heat transfer, *Journal of Mechanical Science and Technology*, Vol. 24, (2010), pp. 1225–1233.
- (16) G.H. Yoon, Topological layout design of electro-fluid-thermal-compliant actuator, *Computer Methods in Applied Mechanics and Engineering*, Vol. 209-212, (2012), pp. 28–44.
- (17) T. Matsumori, T. Kondoh, A. Kawamoto, and T. Nomura, Topology optimization for fluid-thermal interaction problems under constant input power, *Structural and Multidisciplinary Optimization*, Vol. 47, (2013), pp. 571–581.
- (18) C.S. Andreasen, A.R. Gersborg, and O. Sigmund, Topology optimization of microfluidic mixers, *International journal for numerical methods in fluids*, Vol. 61, No. 5, (2009), pp. 498–513.
- (19) G. Marck, M. Nemer, and J. Harion, Topology optimization of heat and mass transfer problems: laminar flow, *Numerical Heat Transfer, Part B: Fundamentals*, Vol. 63, No. 6, (2013), pp. 508–539.
- (20) A.A. Koga, E.C.C. Lopes, H.F. Villa Nova, C.R. de Lima, and E.C.N. Sliva, Development of heat sink device by using topology optimization, *International Journal of Heat and Mass Transfer*, Vol. 64, (2013), pp. 759–772.
- (21) G. Pinggen, A. Evgrafov, K. Maute, Topology optimization of flow domains using the lattice Boltzmann method, *Structural and Multidisciplinary Optimization*, Vol. 34, (2007), pp. 507–524.
- (22) D. Makhijia, G. Pinggen, R. Yang, and K. Maute, Topology optimization of multi-component flows using a multi-relaxation time lattice Boltzmann method, *Computers and Fluids*, Vol. 67, (2012), pp. 104–114.
- (23) S. Kreissl, G. Pinggen, and K. Maute, An explicit level set approach for generalized shape optimization of fluids with the lattice Boltzmann method, *International Journal for Numerical Methods in Fluids*, Vol. 65, (2009), pp. 496–519.
- (24) G. Liu, M. Geier, Z. Liu, M. Krafczyk, and T. Chen, Discrete adjoint sensitivity analysis for fluid flow topology optimization based on the generalized lattice Boltzmann method, *Computers and Mathematics with Applications*, Vol. 68, (2014), pp. 1374–1392.
- (25) K. Yaji, T. Yamada, M. Yoshino, and T. Matsumoto, Topology optimization in thermal fluid flow using the lattice Boltzmann method, *Journal of Computational Physics*, Vol. 307, (2016), pp. 355–377.
- (26) F. Dugas, Y. Favennec, C. Josset, Y. Fan, and L. Luo, Topology optimization of thermal fluid flows with an adjoint Lattice Boltzmann Method, *Journal of Computational Physics*, Vol. 365, (2018), pp. 376–404.
- (27) T. Inamuro, A lattice kinetic scheme for incompressible viscous flows with heat transfer, *Philosophical Transactions of the Royal Society A*, Vol. 360, (2002), pp. 477–484.

- (28) M. Junk and S.V. Raghurama Rao, A new discrete velocity method for Navier-Stokes equations, *Journal of Computational Physics*, Vol. 155. No. 1, (1999), pp. 178–198.
- (29) Y. Sone, *Notes on kinetic-equation approach of fluid-dynamic equations*, Department of Mechanics, Royal Institute of Technology, Stockholm, (2000).
- (30) S. Succi, *The lattice Boltzmann equation for fluid dynamics and beyond*, Oxford University Press, (2001).
- (31) X. He and L.S. Luo, Lattice Boltzmann model for the incompressible Navier-Stokes equation, *Journal of statistical physics*, Vol. 88, (1997), pp. 927–944.
- (32) T. Inamuro, Lattice Boltzmann methods for viscous fluid flows and for two-phase fluid flows, *Fluid Dynamics Research*, Vol. 38, (2006), pp. 641–659.
- (33) T. Yamada, K. Izui, S. Nishiwaki, and A. Takezawa, A topology optimization method based on the level set method incorporating a fictitious interface energy, *Computer Methods in Applied Mechanics and Engineering*, Vol. 199, (2010), pp. 2876–2891.
- (34) K. Yaji, T. Yamada, M. Yoshino, and T. Matsumoto, Topology optimization using the lattice Boltzmann method incorporating level set boundary expressions, *Journal of Computational Physics*, Vol. 274, (2014), pp. 158–181.

